Hindawi Publishing Corporation
Advances in Mechanical Engineering
Volume 2014, Article ID 571063, 8 pages
http://dx.doi.org/10.1155/2014/571063

Research Article

Compressed Biogas-Diesel Dual-Fuel Engine Optimization Study for Ultralow Emission

Hasan Koten, Mustafa Yilmaz, and M. Zafer Gul

Mechanical Engineering Department, Marmara University, 34722 Istanbul, Turkey

Correspondence should be addressed to Hasan Koten; hasan.koten@marmara.edu.tr

Received 2 April 2014; Revised 17 April 2014; Accepted 18 April 2014; Published 2 June 2014

Academic Editor: Jinjia Wei

The aim of this study is to find out the optimum operating conditions in a diesel engine fueled with compressed biogas (CBG) and pilot diesel dual-fuel. One-dimensional (1D) and three-dimensional (3D) computational fluid dynamics (CFD) code and multiobjective optimization code were employed to investigate the influence of CBG-diesel dual-fuel combustion performance and exhaust emissions on a diesel engine. In this paper, 1D engine code and multiobjective optimization code were coupled and evaluated about 15000 cases to define the proper boundary conditions. In addition, selected single diesel fuel (dodecane) and dual-fuel (CBG-diesel) combustion modes were modeled to compare the engine performances and exhaust emission characteristics by using CFD code under various operating conditions. In optimization study, start of pilot diesel fuel injection, CBG-diesel flow rate, and engine speed were optimized and selected cases were compared using CFD code. CBG and diesel fuels were defined as leading reactants using user defined code. The results showed that significantly lower NOx emissions were emitted under dual-fuel operation for all cases compared to single-fuel mode at all engine load conditions.

1. Introduction

In transport industry, compression ignition (CI) engines are highly preferred as power supply compared to spark ignition (SI) engines due to their high thermal efficiency, perfect fuel economy, and low regular emissions of unburned hydrocarbon (UHC), carbon monoxide (CO), and carbon dioxide (CO_2). Biogas-diesel dual-fuel engines commonly exhaust a higher amount of particulate matter (PM) and nitrogen oxide (NOx) pollutant emissions compared to exhaust emission properties of gasoline engines [1–3]. Throughout the recent years, fossil fuels have been affected by a rise in prices of petroleum fuels due to the limitations of deposit and supply and the significant increase in desire of petroleum fuels. Because of PM, NOx and CO_2 emissions cause environment problems, emission regulations for diesel engine strengthened recent years [1, 2]. Therefore, biofuels (liquid and gaseous) have been commonly used for intensive research studies all over the world because they are overestimated as impressively alternative fuels. Biofuels like biogas (gaseous fuel) are renewable, biologically parsable, and biologically the most promising alternative fuels for diesel motors. Biogas is obtained after a fermentation process of renewable agricultural supplies such as animal fats, waste oils, and organic waste. Diesel engine operation can be used with natural gas (NG) and biogas fueling without any modifications. PM (about 70% by mass) and NOx emissions (more than 37% by mass) of dual-fueling tend to be low compared to diesel fueling operating under the same operation [4]. Compressed natural gas (CNG) can be used to lessen noise level, specific fuel consumption, and NOx emissions. However, UHC emission increases for dual-fuel mode which has 75% CNG and 25% diesel fuel [5]. Effects of CNG ratio, advance of pilot injection, intake temperature around the combustion process, emissions, and engine performance of a dual-fueled engine were investigated [6].

In this study, the influence of dual-fuel combustion characteristics to decrease in exhaust emissions along with the combustion performance in the diesel engine fueled with CBG-diesel dual-fuel was investigated. Fire code (AVL), multiobjective optimization code, and 3D Star-CD codes were employed for single diesel fuel (dodecane) and dual-fuel (CBG-diesel) cases. Detailed specifications of engine were given in Table 1. In this work, in-cylinder combustion

Table 1: Engine specifications.

Bore [mm]	76.0
Stroke [mm]	80.5
Displacement volume [cc]	365.25
Number of cylinders	1
Compression ratio	17.6
Air intake	Turbo charged

pressure and rate of heat release (ROHR) were evaluated under different operating conditions and engine loads and we analyzed the combustion characteristics of the CI engine for single-fuel (diesel) and dual-fuel (CBG-diesel) combustions. Moreover, combustion pressure or indicated mean effective pressure (IMEP), exhaust gas temperature, and also soot, NOx, HC, CO, and CO_2 exhaust emissions were investigated under different engine operating conditions to investigate the engine performance and exhaust emission characteristics of single-fuel and dual-fuel modes.

2. Mathematical Modeling

The equations employed to describe mass and momentum can be expressed as

$$\begin{aligned}
&\frac{\partial \rho}{\partial t} + \nabla \cdot (\rho \mathbf{u}) = 0,\\
&\frac{\partial \rho \mathbf{u}}{\partial t} + \nabla \cdot (\rho \mathbf{u}\mathbf{u}) = \nabla P - \nabla \left(\frac{2}{3}\rho k\right) + \nabla \cdot \boldsymbol{\sigma} + \rho g,\\
&\frac{\partial \rho I}{\partial t} + \nabla \cdot (\rho I \mathbf{u}) = -P\nabla \cdot \mathbf{u} - \nabla \left(\frac{2}{3}\rho k\right) + \nabla \cdot \mathbf{J} + \rho\varepsilon,\\
&\frac{\partial}{\partial t}(\rho k) + \nabla \cdot (\rho \mathbf{u} k)\\
&\qquad = -\frac{2}{3}\rho k \cdot \mathbf{u} + \boldsymbol{\sigma} \cdot \nabla \cdot \mathbf{u} + \nabla \left[\left(\frac{\mu_t}{Pr_k}\right)\nabla k\right] - \rho\varepsilon,\\
&\frac{\partial}{\partial t}(\rho\varepsilon) + \nabla \cdot (\rho \mathbf{u}\varepsilon)\\
&\qquad = -\left(\frac{2}{3}c_{\varepsilon 1} - c_{\varepsilon 3}\right)\rho\varepsilon\nabla \cdot \mathbf{u}\\
&\qquad\quad + \nabla \left[\left(\frac{\mu_t}{Pr_\varepsilon}\right)\nabla\varepsilon\right] + \frac{\varepsilon}{k}\left[c_{\varepsilon 1}\boldsymbol{\sigma} : \nabla \mathbf{u} - c_{\varepsilon 2}\rho\varepsilon\right],
\end{aligned} \tag{1}$$

where ρ is the density; P is pressure; $\mathbf{u}$ is the velocity vector; I is specific internal energy; $\boldsymbol{\sigma}$ is the turbulent viscous stress tensor; $\mathbf{J}$ is the heat flux vector including turbulent heat conduction and enthalpy diffusion effects.

Two-equation k-ε models are commonly used for engineering predictions of turbulent flows which provide computational expediency and ease of implementation in finite-volume numerical codes. Their accuracy is generally acceptable only for prediction of mean flow quantities.

Liquid film model predicts the dynamic characteristics of wall films. This is a common phenomenon present in a wide range of situations, such as automotive engines, gas turbines, and spray-cooling systems. A particular example is the port fuel injected (PFI) gasoline engine, where sprays from fuel injectors impinge and form a film on the walls of intake ports, valves, and pistons. The subsequent behavior of the film has a strong influence on mixture preparation, combustion, and emissions. The ability to predict the film's dynamic characteristics is therefore important for the development of such engines. Dispersed multiphase flows are an important feature of IC engine models due to the presence of fuel sprays in such models. In these cases the flow consists of a continuous phase, which may be gaseous or liquid, and one or more dispersed phases in the form of liquid droplets. In general, the motion of the dispersed phase will be influenced by that of the continuous one and vice versa via displacement and interphase momentum, mass, and heat transfer effects. The strength of the interactions will depend on the droplet's size, density, and number density [7].

In particular, the standard k-ε model has been criticized by many researchers as being inaccurate for prediction of recirculating flows and complex shear layers, due to its overdissipative nature. In an attempt to improve the predictive ability of the standard k-ε models, a number of alternatives have been offered [8]. RNG k-ε model, Yakhot-Orszag models, anisotropic k-ε model of Speziale, Morel and Mansour version of the k-ε model, and the k-ω model of Wilcox [9] are well known among turbulence models [9–12]. Three-equation turbulence model has also been offered in order to predict the compressed turbulence in IC engines [13]. Various turbulence models including Chen's k-ε model have been tested and the RNG k-ε model has been chosen for the rest of the simulations [14, 15].

Huh's atomization model was employed in the simulations. This model is based on the premise that the two most important phenomena in spray atomization are the gas inertia and the internal turbulence stresses generated in the nozzle [16].

The fuel particles may become unstable due to the interfacial forces acting on their surfaces during the relative motion according to the continuous phase. This problem was solved by using the break-up model of Reitz and Diwakar. Droplet break-up due to aerodynamic forces exists in two modes in Reitz and Diwakar model [17]. The collision model of O'Rourke was used for interdroplet collisions with the Schmidt and Rutland speed-up algorithm. Moreover, this model includes a coalescence timescale [18–20].

Bai's spray impingement model was used in the simulations as a wall-interaction model for discrete phase. This model was formulated within the framework of the Lagrangian model, which is based on literature findings and mass, momentum, and energy conservation constraints [21]. A random procedure was customized to determine some of the droplet postimpingement quantities to explain the chaotic structure of the impingement process. This allows secondary droplets which are developed from a primary droplet splash to have a distribution of sizes and velocities. The complete model formulation distinguished between dry and wetted wall impingement and is applicable to wall temperatures that are less than the liquid boiling or critical temperature [22, 23].

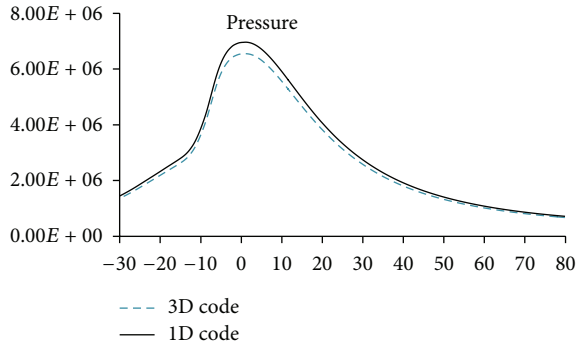

Figure 1: Comparison of 1D and 3D engine code for case 1.

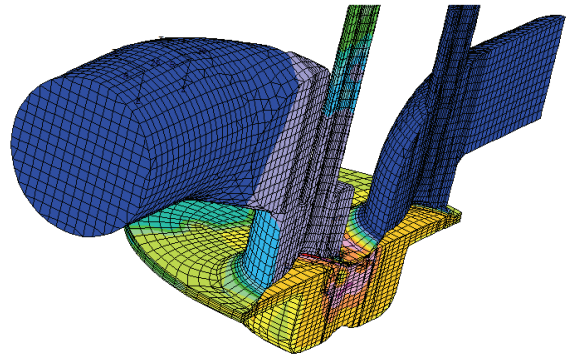

Figure 2: Sectional mesh view for full geometry.

Wiebe function for 1D approximation and extended coherent flame model (ECFM) for 3D CFD solution were used to carry out combustion modeling. 3D engine code was used to find out flow structure in cylinder and behavior of the mixture combustion. 1D engine code was employed to validate 3D results as shown in Figure 1. ECFM and the 3-zone ECFM (ECFM-3Z) broadly belong to the coherent flame model (CFM) family but are extended to nonhomogeneous turbulent premixed and unpremixed (diffusion) combustion. In the ECFM-3Z combustion model, the state of the gases mixture was defined in the 3D space. In addition user defined code was written to define the CBG and diesel fuels as leading reactants.

Soot modeling approach used is based on the laminar flamelet concept in which all scalar quantities are related to the mixture fraction and scalar dissipation rate. Whereas the species mass fractions are unique functions in the mixture fraction-scalar dissipation space, the soot mass fractions are not. The rates of soot formation can, however, be correlated with local conditions in diffusion flames or in partially premixed counter flow twin flames [7].

3. Numerical Methodology and Mesh Generation

The 3D engine code was used to define the piston movement and intake and exhaust valve lifts. It has been exploited to generate the grid to create the hexahedral cells for the engine model including cylinder head, intake and exhaust ports, and piston bowl as shown in Figure 2. The number of cells changed from 500,000 cells in TDC to over 1,700,000 cells in BDC. For the mesh generation hexahedral cells have been accepted since they provided a better accuracy and stability and a less computational time compared to tetrahedral cells.

The notion of moving mesh is that the cell is squeezed to zero volume over one time step, with all its contents (pressure, temperature, mass, momentum, enthalpy, etc.) being expelled into the neighboring cells. Hence, conservation was satisfied exactly even with removal of any cell layer. At the same time, when the cell layers are added, they increase from zero size to their full volume, absorbing the conserved variables through their faces. When the total number of computational cells was over 1,700,000 cells, the typical CPU time taken for the simulation of complete intake, compression, expansion, and exhaust stroke was about 15 hours on a 32 CPU-DELL 7200 workstation with 128 GB system memory. The numerical approximation and computation was based on the pressure-correction method and the PISO algorithm. The second order upwind differencing scheme (MARS) as the spatial discretization was employed for the momentum, energy, and turbulence equations. The temporal discretization was the implicit method, with constant time step. There were high local velocities in the discharge zone and at the beginning and the end of the intake stroke, when the valve lift was quite small. Hence, the time step needed to be small enough as 0.1 and 0.25°CA (on computation) in order to succeed the stability criterion.

4. Optimization Study

Different engine parameters were examined to understand how dual-fuel combustion affects combustion characteristics and exhaust emission in a CI engine. For these cases, start of injection, engine speed, and CBG flow rate were optimized to get proper operating conditions. Selected cases which were obtained by the optimization study were given in Table 2. Detailed investigations of cold flow, spray, and combustion phenomenon for a heavy-duty CI engine were performed by Yilmaz et al. On engine geometry, compression ratio was reduced from 19.75 : 1 to 16.27 : 1 by decreasing maximum radius of the bowl and increasing the depth of the bowl to prevent the immoderately advanced ignition of the premixture formed by early injection

5. Results and Discussions

1D, 3D, and multiobjective optimization codes were employed for single diesel fuel (dodecane) and dual-fuel (CBG-diesel) cases. For both single-fuel and dual-fuel, case 1, case 2, case 3, case 4, and case 5 were investigated at 20%, 40%, 60%, 80%, and 100% engine loads, respectively. The combustion pressures and rates of heat release (ROHR) for the single-fuel mode with diesel fuel in a constant engine speed of 1750 rpm were provided in Figures 3 and 4. The figures showed similar patterns for combustion pressure and ROHR at different engine loads. The combustion pressures and ROHRs increased for both fuels, since engine load increased at constant engine speed. At low engine load

Table 2: Selected cases from optimization process.

Diesel mass (kg/hr)	rpm	SOI (CA bTDC)	NOx (ppm)	Power (kW)	Decision criteria
7.29	1750	−17	65.42	11.89	Power ≥ 11 kW
7.12	1750	−20	57.28	10.47	NOx ≤ 60 ppm

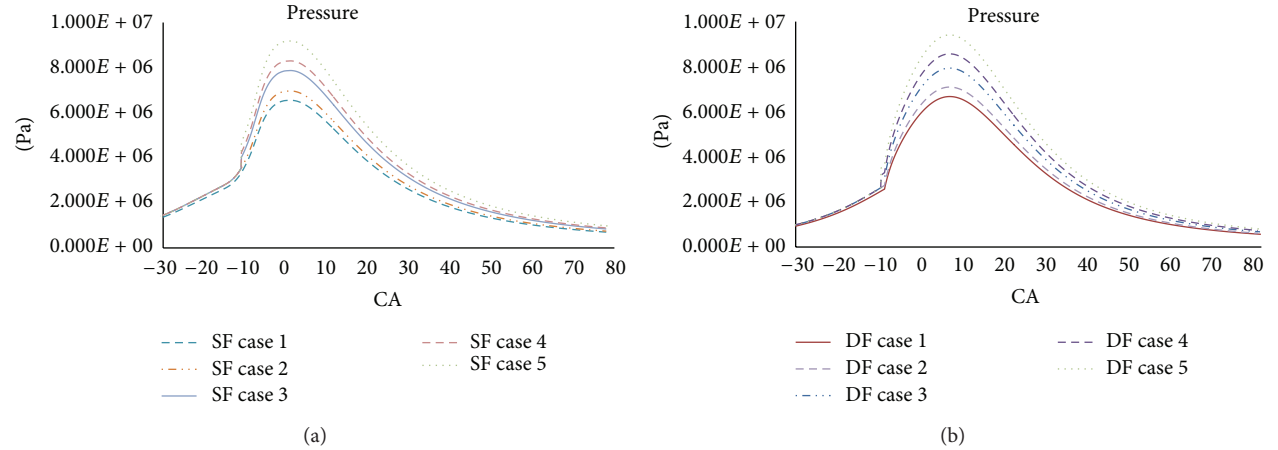

Figure 3: Combustion characteristics at different engine loads. (a) Single-fuel (dodecane) cases. (b) Dual-fuel (CBG-dodecane) cases.

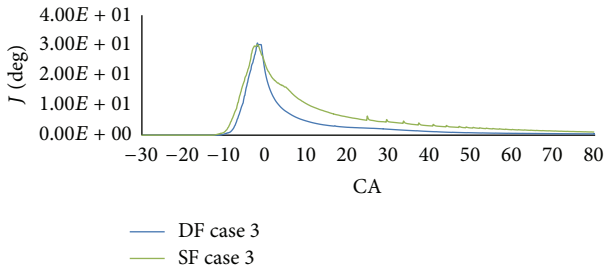

Figure 4: Effect of fuel types on rate of heat release (ROHR) inside cylinder at 60% engine load.

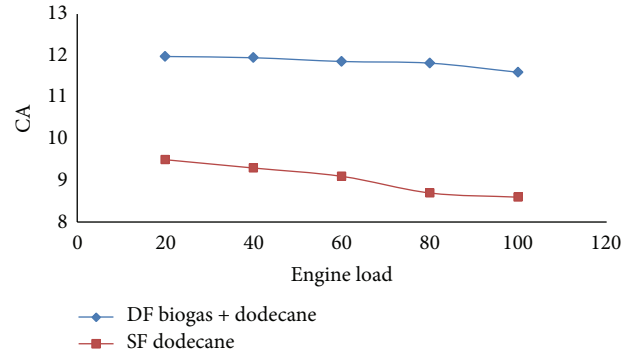

Figure 5: Effect of single- and dual-fuel combustion mode on the ignition delay.

condition (20%), the peak values of combustion pressure and also heat release were slightly lower than other cases as depicted in Figure 3(a). The lower diesel fuel consumption (dodecane, 2.14 kg/h) caused the reduction on the combustion performance. When it came to the 60% load, shown in Figure 3(a), the diesel combustion showed slightly higher peak combustion pressure (P_{max} = 8.4 MPa) and peak heat release compared to CBG-diesel case (P_{max} = 8.3 MPa). Simultaneously, a greater indicated mean effective pressure (IMEP) was obtained for single-fuel diesel injected fuel mass which reached 5.3 kg/h.

However, when compared to start of ignition ability at different engine loads, it was really observed that single-fuel diesel combustion exhibited a slightly shorter ignition delay. Generally, short mixture preparation time results in shorter ignition delay which defines the time between start of injection and start of combustion. The ignition ability in a diesel engine is mainly relying on caffeine and physical fuel properties such as structure of fuel composition, density, bulk module, cetane number, oxygen content, and aromatic content of the fuel [1, 2]. The high cetane number, the reduced stoichiometric air requirement, and the excess oxygen content of air fuel mixture play an important role in short ignition delays for diesel combustion. Effects of dual-fuel and single-fuel combustion on the ROHR were shown in Figure 4 at 60% engine load. In order to investigate the effect of CBG, amount of CBG fuel was changed relating to engine load. Furthermore, fuel mass for pilot fuel was optimized and SOI was adjusted with respect to engine loads in a constant speed of 1750 rpm.

As shown in the figures, the peak combustion pressure and heat release for CBG-diesel dual-fuel combustion are slightly lower compared to single-fuel diesel combustion. In 60% engine load, diesel fuel combustion showed slightly higher peak combustion pressure (P_{max} = 8.55 MPa) and ROHR. Also, ignition delay for single-fuel combustion cases indicated shortened trends in comparison with CBG-diesel dual-fuel cases under all engine loads as shown in Figure 5. In addition, fuel properties of dodecane which has long carbon chain played an important role in short ignition delay. It is observed that dual-fuel and higher CBG fuel concentration increased the ignition delay.

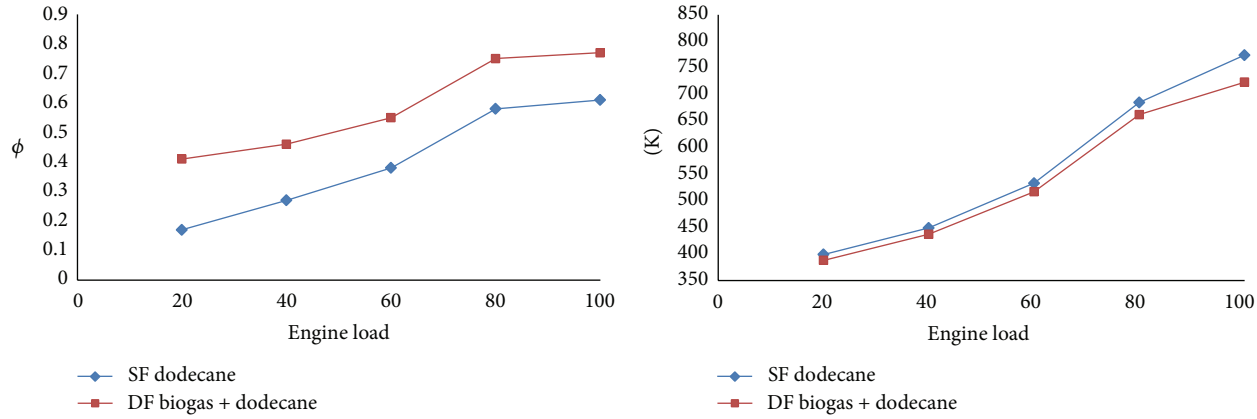

(a) Equivalence ratio

(b) Exhaust average gas temperature

FIGURE 6: Effects of combustion on exhaust gas temperature and equivalence ratio.

For dual-fuel combustion, combustion durations took a long time considerably as well as the increase of pilot and CBG fuel consumption with the increase in engine load with respect to single-fuel combustion mode. These results could be explained by the reduction of oxygen concentration along with the preignition with the ingestion of CBG fuel which caused the deteriorated combustion process and prolonged combustion durations [1, 2]. Moreover, CBG fuel caused slower burning rate, resulting in lengthened combustion durations. Especially, single diesel fuel combustion durations were relatively shorter than other fuel operations due to the difference in cetane number which actively promoted the combustion phase.

Equivalence ratio and exhaust gas temperature results were shown in Figure 6(a) with the variation in engine load. Dual-fuel combustion cases had higher fuel-air equivalence ratios compared to the single-fuel cases. These results were mainly due to the supplied CBG fuel which was combined and replaced with fresh air during the intake process. Furthermore, engine required more fuel to fulfill the imposed engine load-speed condition as engine load was increased and consequently more gaseous fuels need to be injected into the combustion chamber. The relationships between the variation of engine load and exhaust gas temperatures for all fuel modes were provided in Figure 6(b). According to the figures, the exhaust gas temperature showed linearly increased tendency due to the increase in total energy input, when the engine load increased. In addition, exhaust gas temperatures were slightly lower for dual-fuel combustion cases compared to single-fuel mode cases. The difference in exhaust gas temperature could be explained by decreasing charge temperature with CBG ingestion and the delaying combustion phase. Combustion process shifted and retarded to the expansion stroke due to the prolonged ignition delay for dual-fuel cases. These properties caused lower exhaust gas temperature. In this project, single- and dual-fuel combustion performances were also analyzed by means of fuel consumption rate. In the dual-fuel combustion mode, the gaseous fuel (CBG) flow rate and the liquid pilot fuel flow are optimized. The effects of combustion mode and engine load on fuel

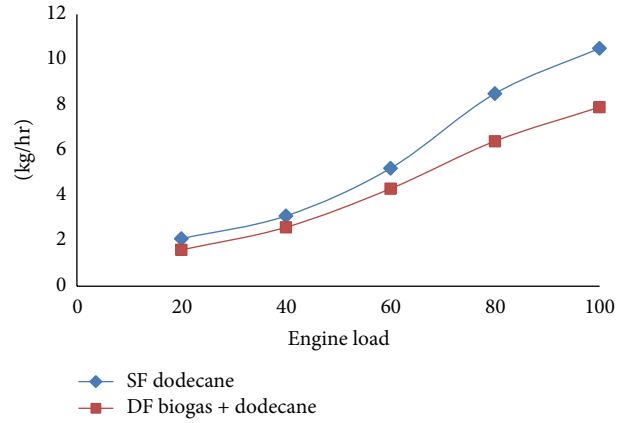

FIGURE 7: Effect of dual-fuel combustion mode on fuel consumption versus engine load.

consumption were shown in Figure 7. In dual-fuel cases, fuel consumption was illustrated for just usage of pilot fuel (dodecane) in Figure 7. At low engine loads, due to the lower air fuel mixture temperature, fuel consumption of diesel fuel increased. Also unburned HC emissions increased due to the lower combustion rate of CBG fuel. In addition, while engine load increases, combustion temperature increases inside the combustion chamber and CBG fuel consumption increases as shown in Figure 7. Moreover, the increase of combustion temperature due to the high CBG fuel consumption resulted in shorter ignition delay at high engine loads.

The concentrations of NOx and soot emissions for the engine operated with single- and dual-fuel combustion modes were shown in Figures 8(a) and 8(b), respectively. In Figure 8(a), when the engine load increased, NOx concentrations of all test cases increased steeply. Significantly lower NOx emissions were emitted within the dual-fuel operations compared to the single mode at all conducted test ranges. In Figure 8(a), single-fuel diesel combustion cases resulted in higher NOx emissions at all engine loads compared to dual-fuel cases. The reason behind this trend could be explained

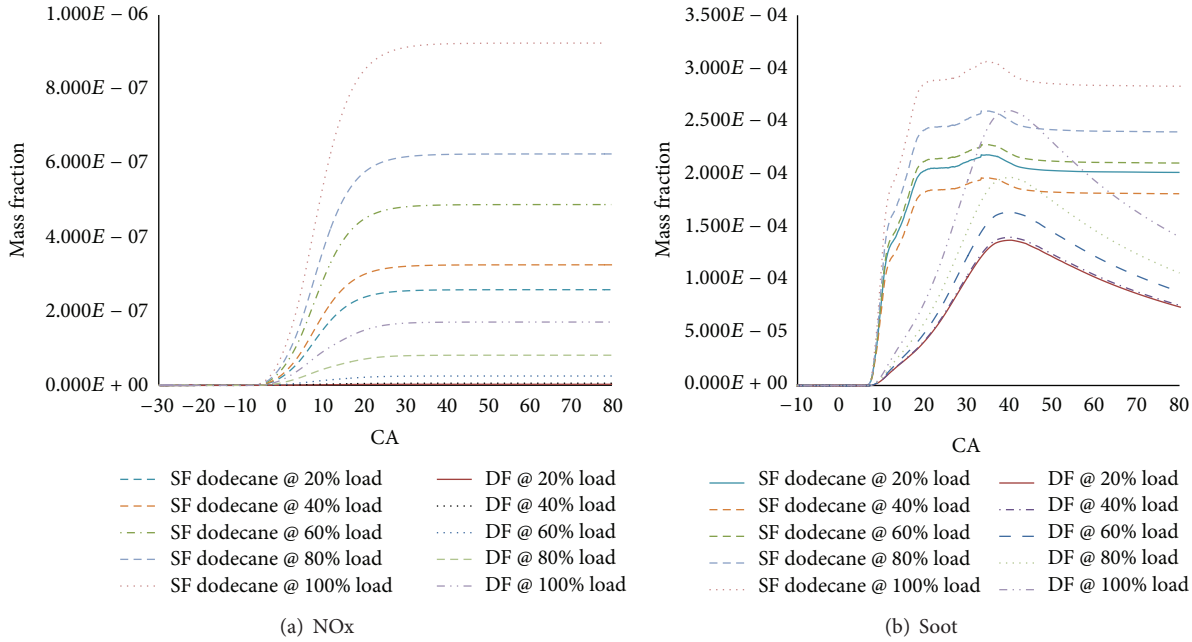

(a) NOx (b) Soot

Figure 8: NOx and soot emissions for single- and dual-fuel cases versus CA. (a) NOx emissions. (b) Soot emissions.

by the faster injection and early ignition characteristics of diesel which are visible in previous outcomes of combustion characteristics.

As shown in Figure 8(b), soot emissions for dual-fuel operations were significantly lower than single-fuel modes. CBG-diesel combustion cases exhibited superior performance in reduction of soot emissions. In soot emissions, this considerable reduction might be caused by the properties of the absence of aromatics which are precursors of soot emissions. In addition, CBG fuel normally needs a lower stoichiometric air which allows complete combustion than dodecane although the oxygen concentration is decreased through the ingestion of CBG. Excess oxygen in single-fuel which promotes more complete combustion played an active role in reduction of soot formation and increase of the oxidation in the soot emission throughout the combustion process. Furthermore, CBG includes no sulfur content and replaced a fraction of liquid fuel and reduced the injected fuel of dodecane in the case of dual-fuel combustion.

In Figures 9(a), 9(b), and 9(c) for single- and dual-fuel cases at various engine loads, CO_2, HC, and CO concentrations were shown. In dual-fuel cases gaseous CBG fuel induced during the intake stroke. This air fuel mixture decreases the charge temperature also affects combustion performance and exhaust emissions. Ignition delay takes longer time in dual-fuel cases because of decrease in charge temperature and lower cetane number. For this reason, in dual-fuel combustion cases, concentrations of HC and CO emissions are bigger than single-fuel cases. In Figure 9(a) HC emissions decreased by increase of engine loads due to the increase of combustion temperature. Similarly, in Figure 9(b) CO concentrations decreased due to the increase of temperature inside the combustion chamber by engine loads. CO_2 content of CBG is ingested during the intake process clearly seen in Figure 9(c). For single-fuel cases, CO_2 emissions are higher than dual-fuel cases when compared to CO_2 content of CBG-dodecane dual-fuel cases. Carbon content of single-fuel cases is relatively higher than dual-fuel cases, resulting in significant increase in CO_2 emissions. As shown in these figures, the concentrations of CO_2 emissions for dual-fuel were obviously under those regarding single diesel combustion modes. Moreover, higher cetane number of diesel and faster injection timing shortened the ignition delay and this reduction is related to a decrease in fuel-rich zone throughout the combustion process [1, 2]. When single- and dual-fuel combustions were compared, the concentrations of HC and CO emissions for the single-fuel mode were considerably lower than dual-fuel mode under all test conditions. CBG-air mixture needs to reach the specific temperature value to continue the flame propagation in the combustion region. CO emissions for single-fuel combustion emitted somewhat lower and roughly constant amounts of soot in comparison to dual-fuel combustion.

6. Conclusions

The combustion performance and characteristics of exhaust emissions were investigated for a CI engine fueled with diesel fuel and CBG fuel under various operating conditions to find out the effects of the dual-fuel combustion. The combustion characteristics of diesel (dodecane) single-fuel and CBG-diesel (dodecane) combustion for 1D and 3D had similar combustion characteristics at various engine loads. In dual-fuel combustion, the peak pressure and ROHR for CBG-diesel dual-fuel were slightly under that relating to dodecane diesel fuel combustion. CBG-diesel dual-fuel combustion showed slightly lower peak ROHR than single-fuel diesel combustion. Also, the ignition delay for single-fuel

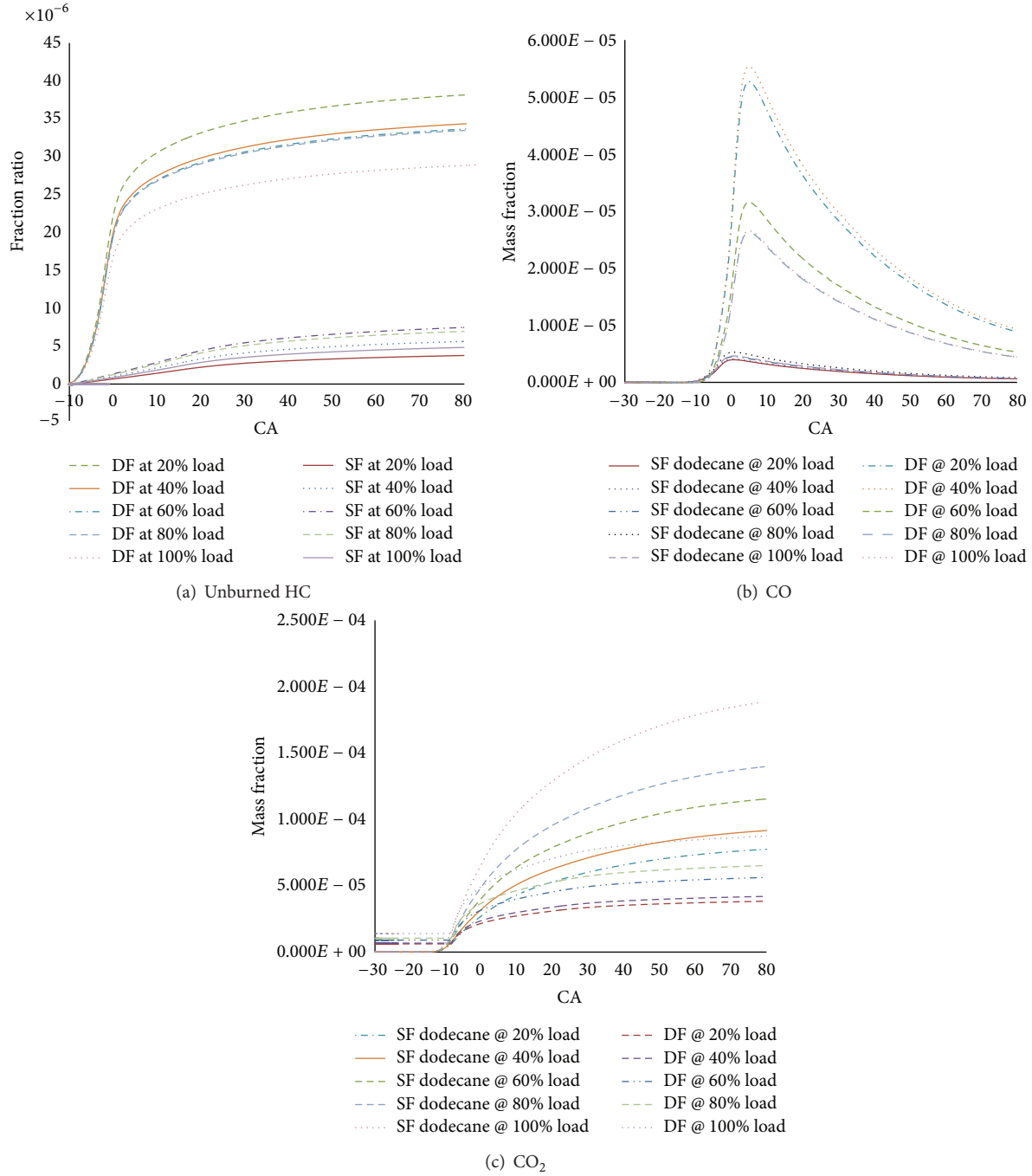

(a) Unburned HC

(b) CO

(c) CO_2

FIGURE 9: Exhaust emissions for single- and dual-fuel cases with different engine loads.

combustion indicated shortened trends in comparison with CBG-diesel dual-fueling due to the high cetane number of diesel fuel.

The ignition delay for dual-fuel cases took a long time with respect to single-fuel cases due to the decrease in charge temperature of CBG-air mixture and high overall specific heat capacity of CBG. Particularly, single-fuel combustion cases were slightly shorter compared to dual-fuel cases under all test conditions due to the short ignition delay, the high cetane number, and also the excess oxygen of mixture. In dual-fuel combustion cases, exhaust gas temperatures were slightly lower compared to single-fuel cases. Low gas temperature was obtained as a result of the delayed combustion process and decreased charge temperature with CBG fuel ingestion during the intake process. At high engine loads (case 4 and case 5), the increase of CBG conversion into work generated a large improvement of the total BSFC. At low engine loads (case 1 and case 2), the absolute fuel consumption for dual-fuel combustion obtained was considerably higher than the single-fuel combustions. Particularly, lower NOx emissions were emitted under the dual-fuel cases compared to the single-fuel mode under all test conditions. In

addition, CBG-diesel cases exhibited superior performance in reduction of soot emissions due to the absence of aromatics and lower stoichiometric air requirement [1, 2]. Concentrations of HC and CO emissions for dual-fuel mode were considerably higher than others under all test conditions. The excess oxygen in air fuel mixture allowed more CO emissions to oxidize into CO_2 in single-fuel combustion cases and resulted in higher concentrations of CO_2 emissions. When CBG was ingested to the cylinder, the CO_2 content in the gas mixture was caused to increase unburned fuel in dual-fuel combustion cases.

Conflict of Interests

The authors declare that there is no conflict of interests regarding the publication of this paper.

Acknowledgments

This work has been supported by Marmara University BAPKO Institution entitled of FEN-C-DRP-101012-0327. The authors would like to thank the BAPKO institution for supporting this research project.

References

[1] M. Y. Kim, S. H. Yoon, and C. S. Lee, "Impact of split injection strategy on the exhaust emissions and soot particulates from a compression ignition engine fueled with neat biodiesel," *Energy and Fuels*, vol. 22, no. 2, pp. 1260–1265, 2008.

[2] M. Y. Kim, S. H. Yoon, J. W. Hwang, and C. S. Lee, "Characteristics of particulate emissions of compression ignition engine fueled with Biodiesel derived from soybean," *Journal of Engineering for Gas Turbines and Power*, vol. 130, no. 5, Article ID 052805, 2008.

[3] R. L. McCormic, C. J. Tennant, R. R. Hayes, and S. Black, "Sharp, regulated emissions from biodiesel tested in heavy duty engines meeting 2004 emission standards," SAE 2005-01-2200, 2005.

[4] N. N. Mustafi and R. R. Raine, "A study of the emissions of a dual fuel engine operating with alternative gaseous fuels," SAE 2008-01-1394, 2008.

[5] S. Maji, A. Pal, and B. B. Arora, "Use of CNG and diesel in CI engines in dual fuel mode," SAE 2008-28-0072, 2008.

[6] S. Jie, Q. Jun, and Y. Mingfa, "Turbocharged diesel/CNG dual-fuel engines with intercooler: combustion, emissions and performance," SAE 2003-01-3082, 2003.

[7] StarCD Manual, "Fuel spray and atomization models," PP. 223–225, 2010.

[8] B. E. Launder and D. B. Spalding, "The numerical computation of turbulent flows," *Computer Methods in Applied Mechanics and Engineering*, vol. 3, no. 2, pp. 269–289, 1974.

[9] D. C. Wilcox, *Turbulence Modeling for CFD*, DCW Industries, 2nd edition, 1998.

[10] V. Yakhot, S. A. Orszag, S. Thangam, T. B. Gatski, and C. G. Speziale, "Development of turbulence models for shear flows by a double expansion technique," *Physics of Fluids A*, vol. 4, no. 7, pp. 1510–1520, 1992.

[11] C. G. Speziale, "On nonlinear k-l and k-ε models of turbulence," *Journal of Fluid Mechanics*, vol. 178, pp. 459–475, 1987.

[12] T. Morel and N. N. Mansour, "Modeling of turbulence in internal combustion engines," SAE Technical Paper Series 820040, 1982, International Congress and Exposition, Detroit, Mich, USA.

[13] M. Z. Gül, *Prediction of in-cylinder flow by use of a multiple time scale turbulence models [Ph.D. thesis]*, University of Manchester, Deptartement of Mechanical Engineering, 1994.

[14] H. Köten, M. Yilmaz, M. Z. Gül, and H. Soyhan, "Comparison of turbulence models for a heavy duty CI engine," ISCSE, 2011.

[15] Y. S. Chen and S. W. Kim, "Computation of turbulent flows using an extended k-ε turbulenceclosure model," NASA CR-179204, 1987.

[16] K. Y. Huh and A. D. Gosman, "A phenomenological model of Diesel spray atomisation," in *Proceedings of the International Conference on Multiphase Flows (ICMF '91)*, pp. 24–27, Tsukuba, Japan, September 1991.

[17] R. D. Reitz and R. Diwakar, "Effect of drop breakup on fuel sprays," SAE Technical Paper Series 860469, 1986.

[18] P. J. O'Rourke, *Collective drop effects on vaporising liquid sprays [Ph.D. thesis]*, University of Princeton, 1981.

[19] D. P. Schmidt and C. J. Rutland, "A new droplet collision algorithm," *Journal of Computational Physics*, vol. 164, no. 1, pp. 62–80, 2000.

[20] M. A. Aamir and A. P. Watkins, "Dense propane spray analysis with a modified collision model," in *Proceedings of the 15th Annual conference on Liquid Atomization and Spray Systems (ILASS-Europe '99)*, pp. 5–7, Toulouse, France, July 1999.

[21] C. Bai and A. D. Gosman, "Development of methodology for spray impingement simulation," SAE Technical Paper Series 950283, 1995.

[22] J.-M. Duclos, M. Zolver, and T. Baritaud, "3D modeling of combustion for DI-SI engines," *Oil and Gas Science and Technology*, vol. 54, no. 2, pp. 259–264, 1999.

[23] M. Yilmaz, H. Koten, and M. Z. Gul, "Effects of the injection parameters of a heavy duty diesel engine," *International Journal of Vehicle Design*, vol. 59, pp. 164–181, 2012.